The ENSO Effect and Asymmetries in Wheat Price Dynamics

David Ubilava*

School of Economics, University of Sydney

This Draft: March 26, 2017

Abstract

Climate has historically played a critical role in the development of nations, primarily due to its intrinsic linkage with agricultural production and prices. This study examines one such relationship between the better known and most talked about climate anomaly, El Niño Southern Oscillation (ENSO), and the international prices of wheat, one of the most produced and consumed grain cereals in the world. The ENSO–price relationship, moreover, is assumed to be characterized by nonlinear dynamics, because of the known asymmetric nature of ENSO cycles, as well as that of wheat prices. This study applies a vector smooth transition autoregressive (VSTAR) modeling framework to monthly spot prices of wheat from the United States, the European Union, Australia, Canada, and Argentina, as well as the sea surface temperature anomalies from the *Nino3.4* region, which serves as a proxy for identifying the ENSO phase. Results show that, overall, wheat prices tend to increase after La Niña events, and decrease after El Niño events. The regime-dependent dynamics are apparent with more amplified price responses after La Niña shocks, and with more persistent price responses during the La Niña conditions. This is consistent with the economics of storage, wherein shocks related to expected supply and demand are known to have a more pronounced effect in a low-inventory regime. Findings of this study have strong implications for development economics, as they point to an additional channel of adversity due to the ENSO-related climate shocks. Moreover, the ENSO-induced price fluctuations are likely to affect the dynamics of international food and cash programs during extreme episodes of this climate anomaly.

Keywords: Asymmetric Dynamics; El Niño Southern Oscillation; International Wheat Prices; Vector Smooth Transition Autoregression.

*E-Mail: david.ubilava@sydney.edu.au

1 Introduction

The El Niño Southern Oscillation (ENSO) is one of the most important, and certainly the most talked-about, *climate anomalies*[1] that can affect economies in many different ways. This quasi-cyclical climate phenomenon occurs in the tropical Pacific, but has global weather implications (Ropelewski and Halpert, 1987; Rosenzweig et al., 2001; Dai, 2013). Owing to these global linkages, also referred to as *teleconnections* (Rasmusson, 1991; Stone et al., 1996; Barlow et al., 2001), ENSO can directly affect the livelihood of many—particularly in the developing world—as high-impact natural disasters, such as droughts, floods, and tropical cyclones, are more likely during its extreme phases (Siegert et al., 2001; Camargo and Sobel, 2005). Moreover, since ENSO can possibly facilitate the co-occurrence of unfavorable weather conditions in different crop-producing regions, an additional channel though which this climate anomaly can affect the well-being of lower-income households is through supply shortages and price spikes of many food and agricultural commodities. These effects, in turn, can amplify food security issues in the short run, as well as impact the well-being of individuals in the long run due to an array of factors, including the reduction in children's intake of nutrients as well as a reduction in the investment in human capital during the economic hardship (FAO, 2011).

The commodity of interest in this study is wheat. Wheat is a grain cereal that is grown on more land than any other crop, and that remains a commodity of vital importance to many in the world (Curtis, 2002). While previous studies have examined the impact of ENSO phase on wheat production (Nicholls, 1985; Legler et al., 1999; Selvaraju, 2003; Iizumi et al., 2014), the effect of this climate phenomenon on wheat price dynamics has remained largely unexplored. The issue is important for a number of reasons, however. First of all, the price spikes are particularly devastating for consumers in lower income countries, which are, moreover, directly vulnerable to climate shocks (Noy, 2009; Bellemare, 2015). Furthermore, ENSO-induced price movements can also alter the terms of trade, and thus negatively affect households (of net importing countries of wheat, in particular) on a macroeconomic level (Bidarkota and Crucini, 2000; Bleaney and Greenaway, 2001). Another channel through which ENSO events may affect the development of

[1] The term "climate anomaly" describes an intermediate-run departure from (long-run) average climate conditions.

nations is through their possible linkage with civil conflicts (Hsiang et al., 2011). A likely causal mechanism of such a relationship is that ENSO-related natural disasters facilitate food shortages and price spikes (Noy, 2009), which are key factors in higher levels of poverty and amplified social unrest (Ivanic et al., 2012; Bellemare, 2015). Notably, the major players in the international wheat market are countries of the developed world, which are also typically involved in various support programs directed to developing nations. Therefore, the fluctuation of wheat prices, in conjunction with production shocks, can affect the opportunity cost, and potentially change the volume (and the value) of international food and cash programs directed to the developing world. The bottom line is that the potential causal relationship between ENSO and commodity price movements may be a critical channel through which this climate anomaly can affect the development of nations and the well-being of those in need. It is, therefore, of the utmost importance to carefully investigate the relationship between ENSO cycles and international wheat prices, and this is the main focus of the current study.

While ENSO can influence the movements of international wheat prices in a number of different ways, the main channel is arguably supply-related. Weather in most of the major wheat-exporting regions, which includes North America, Western Europe, Australia, and Argentina, as well as in two largest producers and consumers of wheat, China and India, is directly affected by the ENSO-related weather shocks. In particular, droughts are common in the northern wheat belt of Australia during El Niño conditions, while La Niña events can cause flooding rains in the region. La Niña events can also induce drier-than-usual conditions in parts of the United States, Argentina and Europe, as well as below normal temperatures in Canada (Dai and Wigley, 2000; Diaz et al., 2001; Bonsal et al., 2001; Taschetto and England, 2009). Weather, of course, is an important factor in crop production (Lobell and Field, 2007; Schlenker and Roberts, 2009; Lobell et al., 2011; Dell et al., 2014). Indeed, the global effect of ENSO on crop production—wheat in particular—has been well identified (Nicholls, 1985; Legler et al., 1999; Iizumi et al., 2014). Iizumi et al. (2014) report that the El Niño conditions result in 1.4 percent reduction, and the La Niña conditions result in 4.0 percent reduction of wheat yield. Wheat prices move in response to the aforementioned supply shocks and—to the extent that wheat is a storable commodity—the level of global wheat stocks

relative to use. For example, the 2010 surge in wheat prices, which coincided with the La Niña episode, was largely attributed to droughts in Russia and China and to floods in Canada and Australia (Algieri, 2014). Bobenrieth et al. (2013) report negative correlations between prices of wheat and its production and stocks-to-use ratios (respectively, -0.33 and -0.40); as well, based on U.S. data, Algieri (2014) suggests almost a one percent increase in wheat prices in response to a one percent reduction in the stocks-to-use ratio.

The foregoing discussion provides a convincing case for the ENSO–price relationship, and also points to the diversified nature of wheat production across time and space. First, there can be offsetting production effects of ENSO in different parts of the world, which may mitigate the price effect of these anomalies. Second, wheat planting and harvesting occurs throughout all the seasons of the year, thus somewhat mitigating the price variability of this commodity (Janzen et al., 2014). In addition to the aforementioned production shocks, ENSO-related weather hazards (e.g., flooding or frosts) may damage infrastructure, and thus interfere with the transportation and timely delivery of grains from a seller to a buyer. Finally, because ENSO has become one of the better-known climate anomalies, economic agents are likely to react to ENSO-related news by taking precautionary measures, thus affecting the supply and demand of stored wheat inventories. All of these will affect the wheat price dynamics.

Quantifying the dynamics of ENSO and wheat prices is an interesting exercise on its own, but this study extends the analysis to also assess the possibly nonlinear relationship between this climate anomaly and prices. Several factors contribute to the belief that the price impacts of ENSO may indeed be nonlinear. First, ENSO cycles are characterized by asymmetric behavior (Hall et al., 2001; Ubilava and Helmers, 2013)—the El Niño-like events develop somewhat abruptly, whereas the La Niña-like conditions develop more gradually. Second, the effect of ENSO events on weather in different parts of the world is also asymmetric (Cai et al., 2010). That is, El Niño and La Niña effects are not mirror images of each other. As such, both El Niño and La Niña shocks may result in lower yields in major wheat-producing regions (Legler et al., 1999; Mason and Goddard, 2001; Iizumi et al., 2014). Finally, the dynamic behavior of wheat prices may also be nonlinear, as commodity price cycles, in general, tend to be asymmetric in their magnitude and

duration (Cashin et al., 2002). This can be linked to the storage behavior, as commodity prices are likely to be more responsive to external shocks—such as new information regarding ENSO events—during the low-inventory regime than in the high-inventory regime (Wright, 2011, 2012). That is, inventories, when available in relative abundance, can facilitate inter-temporal arbitrage and thus moderate the immediate effects of an unanticipated shock. Otherwise, when stocks are low, the market is more susceptible to significant supply drops, and prices spike (Bobenrieth et al., 2013; Algieri, 2014). The foregoing supports the use of a nonlinear modeling framework as a preferred method to properly examine the ENSO-induced wheat price dynamics.

The present paper adopts a vector smooth transition autoregressive (VSTAR) modeling framework to address regime-dependent asymmetries in ENSO and wheat price dynamics (Rothman et al., 2001; Camacho, 2004). VSTAR is a multivariate extension of the smooth transition autoregressive (STAR) model, originally proposed by Chan and Tong (1986) (as the smooth threshold autoregressive model), with the subsequent modeling and testing frameworks developed and popularized in a series of papers by Luukkonen et al. (1988); Teräsvirta and Anderson (1992); Teräsvirta (1994); Eitrheim and Teräsvirta (1996). There are multiple benefits to implementing this modeling technique. First, it is a somewhat generalized framework of nonlinear models, in which is nested the more restricted threshold autoregressive model (Tong and Lim, 1980; Tsay, 1989) as well as the basic linear autoregressive model, as special cases. Second, the smooth transition models also embed elements of other nonlinear techniques, such as Markov switching models (Tyssedal and Tjøstheim, 1988; Hamilton, 1989) and artificial neural networks (Kuan and White, 1994). Finally, the smooth transition modeling framework is readily applicable to address nonlinear commodity price dynamics, and has been successfully used in the literature (Holt and Craig, 2006; Balagtas and Holt, 2009; Goodwin et al., 2011).

A mounting body of literature has examined the relationship between ENSO events and the behavior of agricultural commodity prices. To name a few, Keppenne (1995) reported statistically significant correlation between ENSO phase (especially La Niña) and soybean futures prices. Brunner (2002) found food and agricultural commodity prices to be highly responsive to ENSO variations. Laosuthi and Selover (2007) reported a statistically significant effect of ENSO on price

inflation of maize, sorghum, rice, palm oil, and coconut oil. In a series of papers, Ubilava (2012); Ubilava and Holt (2013); Ubilava (2014) linked price dynamics of major vegetable oils, protein meals, and coffee to ENSO phases. More recently, Algieri (2014) found an increase in U.S. wheat prices due to lower yields associated with La Niña-related weather patterns.

The findings of the present paper contribute to the literature in several key directions. First, this study explores international wheat price dynamics from five major wheat exporting regions in relation to ENSO cycles. Second, this research addresses the potentially causal relationship between ENSO and wheat prices in a nonlinear modeling framework.[2] In so doing, it unveils important linkages between ENSO and wheat prices that can be complex and nontrivial by nature. In particular, this study finds that international wheat prices increase after La Niña shocks at a higher rate than they decrease after El Niño shocks. These effects are most amplified during the first several months following the shocks, and typically dissolve after a one-year period. During the La Niña conditions, however, the price responses are more persistent—a finding that accords with the storage behavior of commodity prices, wherein shocks related to expected production can have more pronounced effect in a low-inventory regime.

2 Econometric Modeling Framework

The modeling exercise of this study relies on a particular kind of nonlinear multivariate framework—the vector smooth transition autoregression (VSTAR). The building block of this model is a basic vector autoregression (VAR). Let $\boldsymbol{x}_t$ be an n-dimensional vector of weakly dependent variables in period t, with a dynamic relationship given by a VAR of order p, VAR(p):

$$\boldsymbol{x}_t = \boldsymbol{\alpha} + \boldsymbol{\Pi}\boldsymbol{d}_t + \sum_{i=1}^{p} \boldsymbol{B}_i \boldsymbol{x}_{t-i} + \boldsymbol{\varepsilon}_t, \tag{1}$$

where $\boldsymbol{\alpha}$ is a vector of constants, $\boldsymbol{\Pi}$ is a matrix of parameters associated with the binary seasonal variable vector $\boldsymbol{d}_t$; $\boldsymbol{B}_i$, $i = 1, \ldots, p$, are n-dimensional matrices of parameters associated with lagged dependent variables; and $\boldsymbol{\varepsilon}_t \sim iid\,(\mathbf{0}, \Sigma_\varepsilon)$, where Σ_ε is the non-diagonal covariance matrix.

[2] Causality here is defined in Granger (1969) sense. That is, the causal variable precedes, and thus can help in predicting the response variable.

Equation (1) can be extended to a nonlinear alternative in many different ways. The present paper employs an additive two-regime nonlinear vector autoregression:

$$\boldsymbol{x}_t = \boldsymbol{\alpha} + \boldsymbol{\Pi}\boldsymbol{d}_t + \sum_{i=1}^{p} \boldsymbol{B}_{0i}\boldsymbol{x}_{t-i} + \boldsymbol{\Gamma}_t \left(\sum_{i=1}^{p} \boldsymbol{B}_{1i}\boldsymbol{x}_{t-i} \right) + \boldsymbol{\varepsilon}_t, \tag{2}$$

where $\boldsymbol{\Gamma}_t = diag\{G_t^1, \ldots, G_t^n\}$ is an n-dimensional diagonal matrix of transition functions, each bounded between 0 and 1, and given by

$$G_t^j = G\left(s_{j,t}; \gamma_j, c_j\right) = \left\{ 1 + \exp\left[-\frac{\gamma_j}{\sigma_{s_j}} (s_{j,t} - c_j) \right] \right\}^{-1}, \quad j = 1, \ldots, n, \tag{3}$$

where $s_{j,t}$ is the regime-switching transition variable associated with equation j in period t, and $\gamma_j > 0$ and c_j are the associated parameters defining the shape of the transition function; σ_{s_j} is the standard deviation of the transition variable. Note that equation (2) assumes linearity in the intercept and seasonal component. That is, the parameters associated with the intercept and seasonal component do not vary with $s_{j,t}$. This need not be the case, but can prove to be a desirable restriction, particularly when a large number of parameters are to be estimated.

Equation (2), coupled with equation (3), results in a variant of the multivariate smooth transition autoregression (van Dijk and Franses, 1999; van Dijk et al., 2002), better known as the logistic vector smooth transition autoregression, or the logistic VSTAR. This is a two-regime potentially smooth transition model, where the transition between the regimes can be gradual or instantaneous (depending on the value of the estimated γ parameter). That is, it offers all the benefits of the vector threshold autoregression with an additional flexibility of allowing a continuum of a "middle ground" between the two regimes (Hubrich and Teräsvirta, 2013). This is a particularly welcome feature in price analysis, considering the heterogeneity of economic agents in terms of their risk aversion and the transaction costs they face (Ubilava and Holt, 2013; Ubilava, 2014). Note that if the γ_j and c_j parameters were known, then the transition function could simply serve as a variable to be interacted with $\boldsymbol{x}_{t-i}$, $i = 1, \ldots, p$, and one could estimate equation (2) using a least squares method. But because the parameters of the transition function also need to be estimated, an iterative nonlinear least squares method (e.g., a variant of the Gauss-Newton algorithm) needs to be

applied. To date, a number of studies have used the multivariate smooth transition autoregressions in general, and (logistic) VSTAR specifications in particular, to tackle various empirical questions (e.g., Weise, 1999; Rothman et al., 2001; Camacho, 2004). For more details on model specification and estimation issues, as well as their peculiarities, refer to Teräsvirta and Yang (2014a) and Teräsvirta and Yang (2014b).

Whether the smooth transition type of nonlinearity—that is, when the parameter vectors are identified in two (or more) regimes between which the transition may be gradual—is an adequate feature of the data generating process, is a testable hypothesis. A conventional approach with the standard test statistics, however, cannot be employed, due to the so-called Davies' problem (Davies, 1977, 1987), which relates to nuisance parameters that are unidentified under the null hypothesis. To illustrate the problem in the current context, consider a single equation of the n-dimensional logistic VSTAR model given by

$$x_{j,t} = \alpha_j + \boldsymbol{\pi}_j' \boldsymbol{d}_t + \sum_{i=1}^{n} \boldsymbol{\beta}_{0i} \boldsymbol{x}_{i,t} + \left(\sum_{i=1}^{n} \boldsymbol{\beta}_{1i} \boldsymbol{x}_{i,t} \right) G\left(s_{j,t}; \gamma_j, c_j\right) + \varepsilon_{j,t} \tag{4}$$

where α_j is a scalar, and $\boldsymbol{\pi}_j$ is a vector of parameters associated with the seasonal dummy variables; $\boldsymbol{x}_{i,t} = (x_{i,t-1}, \ldots, x_{i,t-p})'$, $i = 1, \ldots, n$, is a vector of lagged dependent variables, and $\boldsymbol{\beta}_{0i}$ and $\boldsymbol{\beta}_{1i}$ are the associated parameter vectors; and $G\left(s_{j,t}; \gamma_j, c_j\right)$ is the transition function as described above. At this point, the nonlinear model will reduce to the linear counterpart either by imposing $\gamma_j = 0$, or by setting $\boldsymbol{\beta}_{1i} = \mathbf{0}$, $\forall\, i = 1, \ldots, n$. That is, γ_j and $\boldsymbol{\beta}_{1i}$ are unidentified nuisance parameters that can take any value without affecting the likelihood. As such, the conventional maximum likelihood theory is not directly applicable, which is the essence of the Davies' problem. Luukkonen et al. (1988) proposed a solution to the problem by approximating the transition function, about $\gamma_j = 0$, using the Taylor series expansion, which yields the following auxiliary regression:

$$x_{j,t} = \alpha_j + \boldsymbol{\pi}_j' \boldsymbol{d}_t + \sum_{i=1}^{n} \boldsymbol{\beta}_{0i} \boldsymbol{x}_{i,t} + \sum_{r=1}^{3} \sum_{i=1}^{n} \boldsymbol{\varphi}_{ri} \boldsymbol{x}_{i,t} s_{j,t}^{r} + \upsilon_{j,t} \tag{5}$$

where $s_{j,t}^{r}$, $r = 1, \ldots, 3$, represent a candidate transition variable and the quadratic and cubic terms resulting from the aforementioned Taylor series expansion; also $\upsilon_{j,t}$ combines the original

error term $\varepsilon_{j,t}$ and the approximation error. Conventional testing methods can now be applied to equation (5) to test the null hypothesis: $\boldsymbol{\varphi}_{ri} = \mathbf{0}$, $\forall\ r, i$, which is equivalent to the linearity test against the STAR-type alternative. Note that the foregoing testing framework can be extended to a multivariate setting (e.g., Camacho, 2004), but that will drastically increase number of parameters in the unrestricted model, and the so-called "curse of dimensionality" may distort the standard test (fore further details, see Teräsvirta and Yang, 2014a,b). Therefore, the "equation-by-equation" testing framework is a preferred approach for small and moderate samples.

After the suitable VSTAR model is estimated, the question remains whether the model has successfully absorbed the existing nonlinearities in the data, and moreover (and perhaps more importantly) whether there is evidence for any remaining residual autocorrelation or parameter nonconstancy. The aforementioned testing framework readily incorporates tests of no remaining nonlinearity, no residual autocorrelation, and no structural change. The auxiliary regression setting, as before, is applied where the set of regressors also includes the estimated transition function (and its gradients). See van Dijk et al. (2002) for details.

3 Data

To empirically examine the relationship between ENSO and a set of international wheat prices, the present study used monthly data ranging from January of 1982 to December of 2014. The proxy variable for ENSO is the *Niño3.4* index, collected from the National Oceanic and Atmospheric Administration's Climate Prediction Center.[3] The index is derived from daily sea-surface temperature values interpolated from weekly measures obtained from both satellites and actual locations around the Pacific. The sea-surface temperature anomaly in a given month, then, is the deviation in that particular month from the average historic *Niño3.4* measure relative to the 1981–2010 base period. A substantial positive deviation (i.e., when the anomaly exceeds 0.5°C) implies El Niño conditions, and a comparable negative deviation (i.e., when the anomaly drops below −0.5°C) implies La Niña conditions. Otherwise, i.e., when the index is within the $[-0.5°\text{C}, 0.5°\text{C}]$ band, *normal* or *neutral* conditions are assumed. The index nonetheless, is a continuous variable, and is used in that form

[3] Available online at http://www.cpc.ncep.noaa.gov/data/indices/sstoi.indices.

in the analysis.

The wheat price series are collected from the International Grains Council, and are for the Argentinian (Trigo Pan—Up River), Australian (ASW—Eastern States), Canadian (CWRS—St. Lawrence), the European (France Standard/Grade 1—Rouen), and the United States (HRW—Gulf) markets.[4] The nominal prices are expressed in 2010 U.S. Dollars, using the Producer Price Index (PPI) for all commodities—obtained from the United States Bureau of Labor Statistics—as a deflator. The use of real prices is important, because this accounts for a general increase in commodity prices, i.e., the inflationary effect. Apart from the usual rationale behind the use of real prices (i.e., economic agents, such as producers, consumers, or speculators, base their decisions on relative rather than absolute prices), this paper argues that ENSO may impact the major wheat–producing regions in terms of their decisions regarding international food and cash programs. In this context, it is sensible to use real prices of wheat, as those would be accounted for by donor countries when evaluating assistance programs. The real prices are then transformed to natural logarithms to (i) help mitigate potential heteroskedasticity in the series; (ii) facilitate the interpretation of the impulse-responses in percentage terms; and (iii) avoid any inadequate negative realization of the prices in the out-of-sample simulation analysis. Unlike the ENSO measure, the price series are not mean-centered, as the intercept is left to be accounted for in the regression setting.

The time series of the sea-surface temperature anomaly and wheat prices from the five exporting regions are plotted in Figure 1. Several features of the data are apparent. First, the wheat price series are highly correlated with each other (the correlation coefficients are given in Table 1), and except for the occasional divergences, strongly co-move throughout the sample period. Second, there appears to be a negative correlation between the ENSO cycles and the wheat price cycles. For example, the La Niña episodes of 1988, 2008, and 2011 coincide with wheat price spikes. The relationship between the El Niño episodes and wheat prices does not show up as prominently, however, suggesting that a regime-dependent modeling might indeed be a suitable econometric

[4]Several observations were missing from the data series. In particular, the missing observations accounted for approximately 4.8% of the European wheat, 4.0% of the Argentinian wheat, 3.5% of the Australian wheat, and 2.3% of Canadian wheat prices. The missing observations were recovered by taking a simple average of fitted values from (i) spline interpolation, and (ii) a linear regression on the nearby futures prices of soft red winter wheat as quoted on the Chicago Board of Trade, while controlling for seasonal variation. A reader is referred to the Appendix for further details on this.

technique. Such suitability is a testable hypothesis, as discussed in the next section of the paper.

4 Empirical Framework

In theory, under the assumption of competitive markets, the international prices of homogeneous commodities should be closely linked across the space, that is, spatially integrated. In practice, such linkages are distorted by factors contributing to transaction costs. As such, the prices of internationally traded commodities have lags in their adjustments to new information in markets. The associated price discovery, therefore, is likely to be imperfect and of a dynamic nature (Goodwin and Schroeder, 1991). The transaction costs, moreover, are likely to facilitate an asymmetric adjustment of prices (Meyer and Cramon-Taubadel, 2004). If so, a regime-dependent multivariate modeling framework, such as the VSTAR model, can be a suitbale tool for examining international wheat price dynamics in response to ENSO cycles, which are also characterized by a nonlinear autoregressive behavior (Ubilava and Helmers, 2013).

4.1 The Nonlinear Model Estimation

Let $\boldsymbol{x}_t = (p_t^{\text{USA}}, p_t^{\text{EUR}}, p_t^{\text{AUS}}, p_t^{\text{CAN}}, p_t^{\text{ARG}})'$ represent a vector of real price series of wheat in period t, expressed in natural logarithms; and let z_t be the ENSO measure given by the sea-surface temperature deviations from the average historical temperature in a given month, expressed in degrees Celsius. The goal is to identify a suitable model for examining the dynamics of the ENSO–wheat price relationship, which is achieved in several steps.

First, the order of integration is examined in each considered series. This is done by applying the augmented Dickey–Fuller (ADF) and the Zivot–Andrews (ZA) unit root tests. The latter is particularly relevant when a structural change is suspected in the time series. Both tests consistently reject, in each considered set of prices, the null hypothesis of a unit root, thus suggesting that the time series can be treated as I(0). So the rest of the modeling exercise is carried out using the variables in levels.

Next, the autoregressive lag length is determined jointly within the system of wheat prices and ENSO, based on the multivariate Bayesian Information Criterion (BIC), and subject to no residual

autocorrelation. As a result, the following system of equations was deemed suitable for analyzing the dynamic properties of the ENSO and wheat price series:

$$\boldsymbol{x}_t = \boldsymbol{\alpha} + \boldsymbol{\Pi}\boldsymbol{d}_t + \sum_{i=0}^{4} \boldsymbol{\theta}_i z_{t-i} + \sum_{i=1}^{4} \boldsymbol{B}_i \boldsymbol{x}_{t-i} + \boldsymbol{\varepsilon}_t \tag{6}$$

$$z_t = \delta + \boldsymbol{\pi}'\boldsymbol{d}_t + \sum_{i=1}^{4} \beta_i z_{t-i} + \upsilon_t \tag{7}$$

where z_t is assumed to be a weakly exogenous variable: that is, ENSO contemporaneously affects the wheat prices, but there is no feedback effect from prices to ENSO (also, see Brunner, 2002). Further, $\upsilon_t \sim iid(0, \sigma_\upsilon^2)$ and $\boldsymbol{\varepsilon}_t \sim iid(\mathbf{0}, \Sigma_\varepsilon)$; and the rest are parameters to be estimated.

The selected autoregressive structure, in accordance with convention (Teräsvirta and Anderson, 1992; Rothman et al., 2001; van Dijk et al., 2002), is carried over in the linearity and parameter constancy testing frameworks. The candidate transition variables, for linearity testing, are the lagged values of ENSO, z_{t-l}, where $l = 1, \ldots, p$. The transition variable for parameter constancy testing is t/T, where T is the total length of the time series. The null hypotheses are examined on an equation-by-equation basis, using the auxiliary regressions as in equation (5). In so doing, the approach allows for the possibility of regime-dependent behavior in some, but not necessarily all, price equations. If, based on the linearity test results, nonlinearity appears to be a likely feature of the model dynamics, the smooth transition regression is estimated using a nonlinear least squares algorithm. Alternatively, if there is evidence of structural change, the time-varying regression is estimated in a similar manner. The estimated transition functions, or more precisely, the smoothness and location parameters in the logistic transition functions, are then set as fixed, and the rest of the parameters in the system of equations are re-estimated in a seemingly unrelated regression setting. This last step is necessary, because the current modeling approach allows the transition functions (and thus the right-hand side variables) to vary across the equations. The estimated models are then assessed for no remaining nonlinearity, parameter nonconstancy, or residual autocorrelation.

To preserve the number of degrees of freedom and, to some extent, maintain a parsimony in the price equations, the wheat prices are assumed to be nonlinear in the autoregressive components

only. Subsequently, the following set of nonlinear equations are estimated:

$$\boldsymbol{y}_t = \boldsymbol{\alpha} + \boldsymbol{\Pi}\boldsymbol{d}_t + \sum_{i=0}^{4} \boldsymbol{\theta}_i z_{t-i} + \sum_{i=1}^{4} \boldsymbol{B}_{0i}\boldsymbol{y}_{t-i} + \boldsymbol{\Gamma}_t \left(\sum_{i=1}^{4} \boldsymbol{B}_{1i}\boldsymbol{y}_{t-i} \right) + \boldsymbol{\varepsilon}_t \tag{8}$$

$$z_t = \delta_0 + \pi_0'\boldsymbol{d}_t + \sum_{i=1}^{4} \beta_{0i} z_{t-i} + \left(\delta_1 + \pi_1'\boldsymbol{d}_t + \sum_{i=1}^{4} \beta_{1i} z_{t-i} \right) G_t^{\text{ENSO}} + \upsilon_t \tag{9}$$

where $\boldsymbol{\Gamma}_t = diag\left\{G_t^{\text{USA}}, G_t^{\text{EUR}}, G_t^{\text{AUS}}, G_t^{\text{CAN}}, G_t^{\text{ARG}}\right\}$ is a diagonal matrix of transition functions associated with price equations, and G_t^{ENSO} is the transition function associated with the ENSO equation. These can be functions of the lagged values of ENSO or the time trend, and moreover, some of these transition functions associated with price equations, as discussed previously, may be set to zero. The rest are the variables and parameters defined previously. Note that in equation (8), the ENSO affects the wheat price dynamics through linear as well as nonlinear channels.

The final stage of the estimation process is concerned with model evaluation, which involves testing the adequacy of the estimated models against alternative hypotheses of remaining nonlinearity, structural change, and residual autocorrelation. The framework is similar to that previously described in the context of linearity tests; refer to Teräsvirta (1994) for further details.

4.2 Generalized Impulse–Response Functions

To facilitate the interpretation of the estimated models, this study employs the generalized impulse–response (GIR) functions of Koop et al. (1996), which are particularly suitable for interpreting nonlinear model dynamics. This is because impulse–response functions from nonlinear models are not invariant to the information set (i.e., the history), nor to the magnitude and the direction of the initial shock (i.e., the impulse), or subsequent shocks that occur throughout the response horizon. Consider a GIR at a horizon h:

$$\text{GIR}\left(h, \nu_t, \omega_{t-1}\right) = \mathbb{E}\left(x_{t+h}|\nu_t, \omega_{t-1}\right) - \mathbb{E}\left(x_{t+h}|\omega_{t-1}\right) \tag{10}$$

where $\mathbb{E}(\cdot)$ is an expectation operator. Here ν_t and ω_{t-1} denote the impulse and the history for period t, and are realizations of random variables V_t and Ω_{t-1}, respectively. The GIR, in turn, is

thus a realization of a random variable. That is,

$$\text{GIR}\left(h, V_t, \Omega_{t-1}\right) = \mathbb{E}\left(x_{t+h}|V_t, \Omega_{t-1}\right) - \mathbb{E}\left(x_{t+h}|\Omega_{t-1}\right) \tag{11}$$

Of particular interest are any sign- and history-specific asymmetries. Sign-specific asymmetries can be obtained by conditioning the GIR on the subset of shocks (say, only positive shocks or only negative shocks). For example, the GIRs associated with positive shocks are given by

$$\text{GIR}\left(h, \nu_t^+, \Omega_{t-1}\right) = \mathbb{E}\left(x_{t+h}|\nu_t \in V_t^+, \Omega_{t-1}\right) - \mathbb{E}\left(x_{t+h}|\Omega_{t-1}\right) \tag{12}$$

where V_t^+ denotes the subset of positive impulses. Similarly, the GIRs associated with negative shocks, $\text{GIR}\left(h, \nu_t^-, \Omega_{t-1}\right)$, are obtained using the subset of negative impulses. A sign-specific asymmetry would imply $\text{GIR}\left(h, \nu_t^+, \Omega_{t-1}\right) \neq \text{GIR}\left(h, \nu_t^-, \Omega_{t-1}\right)$, for some h, where $\nu_t^+ = -\nu_t^-$.

A history-specific asymmetry can be illustrated by comparing the GIRs that are associated with different subsets of histories, Ω_{t-1}^r (e.g., $r = 1, 2$), each obtained by

$$\text{GIR}\left(h, V_t, \omega_{t-1}^r\right) = \mathbb{E}\left(x_{t+h}|V_t, \omega_{t-1} \in \Omega_{t-1}^r\right) - \mathbb{E}\left(x_{t+h}|\omega_{t-1} \in \Omega_{t-1}^r\right) \tag{13}$$

More to the point, this study aims to find any sign-specific asymmetries due to the "El Niño-like surprises" and "La Niña-like surprises", given respectively by positive and negative ENSO shocks of similar magnitude, as well as any history-specific asymmetries in the wheat price dynamics in two extreme regimes, identified as the "La Niña regime"—that is, when the sea-surface temperature anomaly (SSTA) is less than -0.5°C, and the "El Niño regime"—that is, when the SSTA is greater than 0.5°C.

To obtain the GIRs associated with ENSO shocks, this study applies a bootstrap resampling method outlined in Koop et al. (1996). Because ENSO is modeled as a weakly exogenous variable, first the future realizations of ENSO are simulated, which are then incorporated into the system of price equations to generate iterated paths of wheat price realizations over the length of forecast horizon and, subsequently, the impulse–response functions.

That is, in the first step, for a randomly sampled history, ω_{t-1}, an h-step-ahead bootstrap extrapolate of ENSO is obtained based on the available information at the time, and a set of idiosyncratic shocks, $\{\varepsilon^b_{t+h} : h = 1, 2, \ldots\}$, which are randomly sampled from the pool of the estimated residuals:

$$z^b_{t+h} = f\left(z^b_{t+h-1}, \ldots, z_t, z_{t-1}, \ldots; \hat{\theta}\right) + \varepsilon^b_{t+h} \tag{14}$$

where $f(\cdot)$ represents the functional form of the estimated model (viz., the smooth transition autoregressive model in the current case) and $\hat{\theta}$ is a vector of parameter estimates. In effect, $\{z^b_{t+h} : h = 1, 2, \ldots\}$ is an iterated path of future ENSO realizations disturbed by idiosyncratic shocks. In addition, another iterated path of ENSO realizations is obtained in a similar manner, with an exception that at zero horizon, the realization of ENSO is disturbed by an impulse, ν_t:

$$z^b_{t+h|\nu_t} = f\left(z^b_{t+h-1|\nu_t}, \ldots, z_t + \nu_t, z_{t-1}, \ldots; \hat{\theta}\right) + \varepsilon^b_{t+h} \tag{15}$$

These two bootstrap extrapolates are then separately incorporated into the price equations to iterate forward the wheat prices with and without initial ENSO shock:

$$\boldsymbol{y}^b_{t+h} = g\left(\boldsymbol{y}^b_{t+h-1}, \ldots, \boldsymbol{y}_t, \boldsymbol{y}_{t-1}, \ldots, z^b_{t+h}, \ldots, z_t, z_{t-1}, \ldots; \hat{\Theta}\right) + \boldsymbol{v}^b_{t+h} \tag{16}$$

$$\boldsymbol{y}^b_{t+h|\nu_t} = g\left(\boldsymbol{y}^b_{t+h-1|\nu_t}, \ldots, \boldsymbol{y}_t, \boldsymbol{y}_{t-1}, \ldots, z^b_{t+h|\nu_t}, \ldots, z_t + \nu_t, z_{t-1}, \ldots; \hat{\Theta}\right) + \boldsymbol{v}^b_{t+h} \tag{17}$$

where $g(\cdot)$ represents the estimated vector smooth transition autoregressive model and $\hat{\Theta}$ is an array of the associated parameter estimates.

For a total of $B = 500$ such bootstrap extrapolates, generalized impulse–response functions are computed by taking the difference between the simple averages of the forward iterated paths with and without an initial ENSO shock:

$$\mathrm{GIR}_x\left(h, \nu_t, \omega_{t-1}\right) = B^{-1}\sum_{b=1}^{B} x^b_{t+h|\nu} - B^{-1}\sum_{b=1}^{B} x^b_{t+h} \tag{18}$$

These GIRs are generated using 50 randomly sampled histories and 21 initial shocks. The histories

are sampled either from the complete set, or the subset associated with each of the extreme ENSO regimes. The initial shocks are assigned values of $\nu_t = \pm 1.0\sigma_\nu, \pm 1.1\sigma_\nu, \ldots, \pm 3.0\sigma_\nu$. Thus for each scenario—that is, the positive and negative ENSO shocks within the complete set of histories, as well as the subsets of histories associated with the El Niño and the La Niña regimes—a total of 1050 GIRs are generated, which is a sufficiently large sample to help approximate the densities at each horizon across all histories and initial shocks in consideration.

5 Results and Discussion

To reiterate, the nonlinear model estimation is a three-step process that involves model selection, model fitting, and model evaluation. Related to the first step, the linearity and parameter constancy test results are presented in Table 3. To test linearity, up to and including four lags of the ENSO as candidate transition variables are used; to test parameter constancy, a normalized trend, $t^* = t/T$, is applied as per convention. The tests reveal strong evidence of regime-dependent nonlinearities in the ENSO as well as the U.S. and Canadian wheat price equations. In addition, the tests suggest the possibility of a structural change in the European and Australian wheat price dynamics.[5] Therefore, a nonlinear model featured in equations (8) and (9) is fit following the algorithm outlined in the previous section.

Table 4 summarizes the estimated transition functions. Note that in several instances the standard errors associated with the parameter estimates are not provided. These are the cases where either the smoothness parameter, γ, was set to be 100, in effect, implying an instantaneous switch between the regimes; or where the location parameter, c, was set to be equal to a certain point (e.g., 15^{th} percentile of the transition variable).

The estimated transition functions are better illustrated in Figure 2. First consider the transition functions associated with the lagged ENSO realization. The transition between the regimes is indeed gradual in the ENSO equation and the Canadian wheat prices (Panels 2a and 2e). The in-

[5] While in the considered time-frame, the present study found no evidence of structural change in the ENSO cycle, several recent studies (that apply longer time series of this climate anomaly) have reported the impacts of climate change on mean sea-surface temperatures, as well as on increased probability of extreme ENSO phases (Li et al., 2011; Cai et al., 2014, 2015). Addressing the implications of climate change on the ENSO – price relationship may be an interesting avenue for future research.

flection point of the transition function in the ENSO equation is centered about neutral conditions, with distinct autoregressive dynamics in El Niño and La Niña regimes. The Canadian wheat price equation features a smooth transition between the "extreme" La Niña regime, neutral conditions, and the El Niño regime. Such a gradual switch between the two regimes is perhaps indicative of the probabilistic nature of ENSO-induced weather shocks. For example, La Niña-like conditions would imply a worse than average crop, and thus typically are characterized by increased prices. But it takes an extreme La Niña realization—such as the 1988–1989 La Niña or the 2007–2008 La Niña—for a price spike to occur. In the case of the U.S. wheat price equation, however, the switch between the two regimes happens instantaneously in the neighborhood of neutral conditions (Panel 2b), suggesting that the prices respond differently to positive and negative ENSO shocks.

In terms of the structural change, the European wheat price dynamics appear to have altered abruptly at around 2002 (Panel 2c), while the gradual switch between the regimes concluded at around 2007 for the Australian wheat prices (Panel 2d). A potential cause for the former is, perhaps, a change in the grading system, which took effect in the early 2000s (quoted as "Standard Grade" prior to 2002, and "Grade 1" afterwards). As for the Australian prices, the structural change can be attributed to the 2008 deregulation of bulk wheat exports, and the anticipatory build-up in the preceding years.

Finally, the modeling cycle is completed by evaluating the estimated models for no remaining nonlinearity, parameter nonconstancy, and residual autocorrelation. Table 3 features these test results, by and large confirming the adequacy of the estimated models.

The dynamic properties of the estimated model are better illustrated via the generalized impulse–response functions outlined in the previous section. The mean paths for the GIRs associated with positive and negative ENSO shocks, and unconditional on histories, are presented in Figure 3. Several features of interest are notable. First, the La Niña shocks result in increased wheat prices, while the El Niño shocks facilitate price decreases. The price effect of an ENSO shock reaches its maximum after about six-to-ten months. The GIRs range between two-to-six percent in magnitude, and are statistically significant up until the ten-month horizon.

The other interesting feature of the observed dynamics is that the GIRs after a positive shock are

not mirror images of the GIRs after a negative shock. The sign-specific asymmetries are particularly apparent in the case of Canadian wheat: the prices increase at a higher rate (up to five percentage points) after the La Niña shock, but decrease at a considerably lower rate (about two andone-half percentage points) after the El Niño shock.

In addition, two more sets of GIRs are generated, each conditioned on a subset of histories, defined as the La Niña and the El Niño regimes. These GIRs (see Figures 4 and 5) reveal additional interesting characteristics that complement the previously observed dynamics. First, the ENSO impulse–responses confirm a relatively swift mean-reversion during the El Niño regime, but a less amplified adjustment to the long-run mean—with an indication of the so-called "double-dip"—during the La Niña conditions. Subsequently, the price dynamics are also characterized by more persistent behavior in response to ENSO shocks during La Niña conditions. This finding is consistent with the economics of storage (Wright, 2011, 2012). If the global weather conditions associated with a La Niña episode have a net negative global impact on wheat production, the international grain reserves will deteriorate. In such a low-inventory regime, any further ENSO-induced shocks (or ENSO-related news) will result in more amplified price responses.

6 Conclusion

Using more than three decades of monthly data, this study examines ENSO-induced asymmetric price transmissions in the international wheat market. In so doing, it quantifies a rather nontrivial link between the ENSO-related supply shocks and the subsequent wheat price fluctuations. The key findings of this study suggest that ENSO indeed affects international wheat prices, and more interestingly, there are ENSO-related regime-dependencies in the price dynamics. A positive ENSO shock (El Niño) results in decreased wheat prices, while a negative ENSO shock (La Niña) results in increased wheat prices. The impacts of ENSO to wheat prices vary across the considered export regions, but are all within five to six percent magnitude in the intermediate run. Due to asymmetries, the price impact of La Niña is (in absolute terms) larger than the price impact of El Niño, which is consistent with previous findings related to the global production effect of the two extreme phases of ENSO (Iizumi et al., 2014). In addition, this study finds that price responses are more

pronounced during La Niña conditions than during El Niño conditions, possibly identifying the increased responsiveness of a the prices of a storable commodity in a low-inventory regime (Wright, 2012)—a finding that is also consistent with that of Algieri (2014).

This study contributes to the growing literature in the economics of climate anomalies. The key findings are of particular appeal to development economics because climate and its anomalies play a crucial role in the development of nations. These findings can gain additional importance with climate change, as a warmer climate is likely to enhance ENSO variability and facilitate more extreme weather events around the globe (Collins et al., 2010; Li et al., 2011; Cai et al., 2014, 2015). Furthermore, while wheat is one of the most produced and consumed cereals around the world, many wheat-exporting countries are heavily involved in international food aid programs (e.g., Nunn and Qian, 2014), and it appears that the opportunity cost of the aid may increase after the La Niña shocks. In the wake of the ongoing discussion related to the effectiveness of different international aid programs (Lentz et al., 2013), the findings of this study thus offer additional insights to facilitate the discussion of the global economic effect of climate anomalies. Overall, this study improves understanding of the economic impact of ENSO, which can be a valuable tool in mitigating the adverse effects of climate anomalies, particularly in the developing world.

References

Algieri, B. (2014). A Roller Coaster Ride: An Empirical Investigation of the Main Drivers of the International Wheat Price. *Agricultural Economics 45*(4), 459–475.

Balagtas, J. V. and M. T. Holt (2009). The Commodity Terms of Trade, Unit Roots, and Nonlinear Alternatives: A Smooth Transition Approach. *American Journal of Agricultural Economics 91*(1), 87–105.

Barlow, M., S. Nigam, and E. Berbery (2001). ENSO, Pacific Decadal Variability, and US Summertime Precipitation, Drought, and Stream Flow. *Journal of Climate 14*(9), 2105–2128.

Bellemare, M. F. (2015). Rising Food Prices, Food Price Volatility, and Social Unrest. *American Journal of Agricultural Economics 97*(1), 1–21.

Bidarkota, P. and M. J. Crucini (2000). Commodity Prices and the Terms of Trade. *Review of International Economics 8*(4), 647–666.

Bleaney, M. and D. Greenaway (2001). The Impact of Terms of Trade and Real Exchange Rate Volatility on Investment and Growth in Sub-Saharan Africa. *Journal of Development Economics 65*(2), 491–500.

Bobenrieth, E., B. Wright, and D. Zeng (2013). Stocks-to-use Ratios and Prices as Indicators of Vulnerability to Spikes in Global Cereal Markets. *Agricultural Economics 44*(s1), 43–52.

Bonsal, B. R., A. Shabbar, and K. Higuchi (2001). Impacts of Low Frequency Variability Modes on Canadian Winter Temperature. *International Journal of Climatology 21*(1), 95–108.

Brunner, A. (2002). El Nino and World Primary Commodity Prices: Warm Water or Hot Air? *Review of Economics and Statistics 84*(1), 176–183.

Cai, W., S. Borlace, M. Lengaigne, P. Van Rensch, M. Collins, G. Vecchi, A. Timmermann, A. Santoso, M. J. McPhaden, L. Wu, M. H. England, G. Wang, E. Guilyardi, and F.-F. Jin (2014). Increasing Frequency of Extreme El Niño Events Due to Greenhouse Warming. *Nature Climate Change 4*(2), 111–116.

Cai, W., P. Van Rensch, T. Cowan, and A. Sullivan (2010). Asymmetry in ENSO Teleconnection with Regional Rainfall, its Multidecadal Variability, and Impact. *Journal of Climate 23*(18), 4944–4955.

Cai, W., G. Wang, A. Santoso, M. J. McPhaden, L. Wu, F.-F. Jin, A. Timmermann, M. Collins, G. Vecchi, M. Lengaigne, M. H. England, D. Dommenget, K. Takahashi, and E. Guilyardi (2015). Increased Frequency of Extreme La Niña Events Under Greenhouse Warming. *Nature Climate Change 5*(2), 132–137.

Camacho, M. (2004). Vector Smooth Transition Regression Models for US GDP and the Composite Index of Leading Indicators. *Journal of Forecasting 23*(3), 173–196.

Camargo, S. J. and A. H. Sobel (2005). Western North Pacific Tropical Cyclone Intensity and ENSO. *Journal of Climate 18*(15), 2996–3006.

Cashin, P., C. J. McDermott, and A. Scott (2002). Booms and Slumps in World Commodity Prices. *Journal of Development Economics 69*(1), 277–296.

Chan, K. and H. Tong (1986). On Estimating Thresholds in Autoregressive Models. *Journal of Time Series Analysis 7*(3), 179–190.

Collins, M., S.-I. An, W. Cai, A. Ganachaud, E. Guilyardi, F.-F. Jin, M. Jochum, M. Lengaigne, S. Power, A. Timmermann, G. Vecchi, and A. Wittenberg (2010). The Impact of Global Warming on the Tropical Pacific Ocean and El Niño. *Nature Geoscience 3*(6), 391–397.

Curtis, B. C. (2002). Wheat in the World. In B. C. Curtis, S. Rajaram, and H. G. Macpherson (Eds.), *Bread Wheat: Improvement and Production*, Number 30 in FAO Plant Production and Protection Series. Rome: Food and Agriculture Organization of the United Nations.

Dai, A. (2013). Increasing Drought under Global Warming in Observations and Models. *Nature Climate Change 3*(1), 52–58.

Dai, A. and T. Wigley (2000). Global Patterns of ENSO-induced Precipitation. *Geophysical Research Letters 27*(9), 1283–1286.

Davies, R. (1977). Hypothesis Testing when a Nuisance Parameter is Present only under the Alternative. *Biometrika 64*(2), 247–254.

Davies, R. (1987). Hypothesis Testing when a Nuisance Parameter is Present only under the Alternative. *Biometrika 74*(1), 33–43.

Dell, M., B. F. Jones, and B. A. Olken (2014). What Do We Learn from the Weather? The New Climate-Economy Literature. *Journal of Economic Literature 52*(3), 740–798.

Diaz, H. F., M. P. Hoerling, and J. K. Eischeid (2001). ENSO Variability, Teleconnections and Climate Change. *International Journal of Climatology 21*(15), 1845–1862.

Eitrheim, O. and T. Teräsvirta (1996). Testing the Adequacy of Smooth Transition Autoregressive Models. *Journal of Econometrics 74*(1), 59–75.

FAO (2011). *The State of Food Insecurity in The World: How Does International Price Volatility Affect Domestic Economies and Food Security?* Food & Agriculture Organization of the United Nations.

Goodwin, B. K., M. T. Holt, and J. P. Prestemon (2011). North American Oriented Strand Board Markets, Arbitrage Activity, and Market Price Dynamics: A Smooth Transition Approach. *American Journal of Agricultural Economics 93*(4), 993–1014.

Goodwin, B. K. and T. C. Schroeder (1991). Price Dynamics in International Wheat Markets. *Canadian Journal of Agricultural Economics 39*(2), 237–254.

Granger, C. W. (1969). Investigating Causal Relations by Econometric Models and Cross-Spectral Methods. *Econometrica 37*(3), 424–438.

Hall, A., J. Skalin, and T. Teräsvirta (2001). A Nonlinear Time Series Model of El Niño. *Environmental Modelling & Software 16*(2), 139–146.

Hamilton, J. D. (1989). A New Approach to the Economic Analysis of Nonstationary Time Series and the Business Cycle. *Econometrica 57*(2), 357–384.

Holt, M. T. and L. A. Craig (2006). Nonlinear Dynamics and Structural Change in the U.S. Hog-Corn Cycle: A Time-Varying STAR Approach. *American Journal of Agricultural Economics 88*(1), 215–233.

Hsiang, S., K. Meng, and M. Cane (2011). Civil Conflicts are Associated with the Global Climate. *Nature 476*(7361), 438–441.

Hubrich, K. and T. Teräsvirta (2013). Thresholds and Smooth Transitions in Vector Autoregressive Models. Research Paper 13, CREATES.

Iizumi, T., J.-J. Luo, A. J. Challinor, G. Sakurai, M. Yokozawa, H. Sakuma, M. E. Brown, and T. Yamagata (2014). Impacts of El Niño Southern Oscillation on the Global Yields of Major Crops. *Nature Communications 5*(3712).

Ivanic, M., W. Martin, and H. Zaman (2012). Estimating the Short-Run Poverty Impacts of the 2010–11 Surge in Food Prices. *World Development 40*(11), 2302–2317.

Janzen, J., C. A. Carter, A. Smith, and M. Adjemian (2014). Deconstructing Wheat Price Spikes: A Model of Supply and Demand, Financial Speculation, and Commodity Price Comovement. ERR-165, U.S. Department of Agriculture, Economic Research Service. April, 2014.

Keppenne, C. (1995). An ENSO Signal in Soybean Futures Prices. *Journal of Climate 8*(6), 1685–1689.

Koop, G., M. Pesaran, and S. Potter (1996). Impulse Response Analysis in Nonlinear Multivariate Models. *Journal of Econometrics 74*(1), 119–147.

Kuan, C.-M. and H. White (1994). Artificial Neural Networks: An Econometric Perspective. *Econometric Reviews 13*(1), 1–91.

Laosuthi, T. and D. D. Selover (2007). Does El Niño Affect Business Cycles? *Eastern Economic Journal 33*(1), 21–42.

Legler, D., K. Bryant, and J. O'Brien (1999). Impact of ENSO-related Climate Anomalies on Crop Yields in the U.S. *Climatic Change 42*(2), 351–375.

Lentz, E. C., S. Passarelli, and C. B. Barrett (2013). The Timeliness and Cost-Effectiveness of the Local and Regional Procurement of Food Aid. *World Development 49*, 9–18.

Li, J., S.-P. Xie, E. R. Cook, G. Huang, R. D'Arrigo, F. Liu, J. Ma, and X.-T. Zheng (2011). Interdecadal Modulation of El Niño Amplitude During the Past Millennium. *Nature Climate Change 1*(2), 114–118.

Lobell, D. B. and C. B. Field (2007). Global Scale Climate – Crop Yield Relationships and the Impacts of Recent Warming. *Environmental Research Letters 2*(1), 1–7.

Lobell, D. B., W. Schlenker, and J. Costa-Roberts (2011). Climate Trends and Global Crop Production Since 1980. *Science 333*(6042), 616–620.

Luukkonen, R., P. Saikkonen, and T. Teräsvirta (1988). Testing Linearity Against Smooth Transition Autoregressive Models. *Biometrika 75*(3), 491–499.

Mason, S. J. and L. Goddard (2001). Probabilistic precipitation anomalies associated with ENSO. *Bulletin of the American Meteorological Society 82*(4), 619–638.

Meyer, J. and S. Cramon-Taubadel (2004). Asymmetric Price Transmission: A Survey. *Journal of Agricultural Economics 55*(3), 581–611.

Nicholls, N. (1985). Impact of the Southern Oscillation on Australian Crops. *Journal of Climatology 5*(5), 553–560.

Noy, I. (2009). The Macroeconomic Consequences of Disasters. *Journal of Delopment Economics 88*(2), 221–231.

Nunn, N. and N. Qian (2014). US Food Aid and Civil Conflict. *The American Economic Review 104*(6), 1630–1666.

Rasmusson, E. (1991). *Teleconnections Linking Worldwide Climate Anomalies*, Chapter Observational Aspects of ENSO Cycle Teleconnections, pp. 309–343. Cambridge University Press, New York.

Ropelewski, C. and M. Halpert (1987). Global and Regional Scale Precipitation Patterns Associated with the El Niño/Southern Oscillation. *Monthly Weather Review 115*(8), 1606–1626.

Rosenzweig, C., A. Iglesias, X. Yang, P. R. Epstein, and E. Chivian (2001). Climate Change and Extreme Weather Events: Implications for Food Production, Plant Diseases, and Pests. *Global Change & Human Health 2*(2), 90–104.

Rothman, P., D. van Dijk, and P. H. Franses (2001). Multivariate STAR Analysis of Money–Output Relationship. *Macroeconomic Dynamics 5*(4), 506–532.

Schlenker, W. and M. J. Roberts (2009). Nonlinear Temperature Effects Indicate Severe Damages to U.S. Crop Yields under Climate Change. *Proceedings of the National Academy of Sciences 106*(37), 15594–15598.

Selvaraju, R. (2003). Impact of El Niño–Southern Oscillation on Indian Foodgrain Production. *International Journal of Climatology 23*(2), 187–206.

Siegert, F., G. Ruecker, A. Hinrichs, and A. Hoffmann (2001). Increased Damage from Fires in Logged Forests during Droughts Caused by El Niño. *Nature 414*(6862), 437–440.

Stone, R., G. Hammer, and T. Marcussen (1996). Prediction of Global Rainfall Probabilities Using Phases of the Southern Oscillation Index. *Nature 384*(6606), 252–255.

Taschetto, A. S. and M. H. England (2009). El Niño Modoki Impacts on Australian Rainfall. *Journal of Climate 22*(11), 3167–3174.

Teräsvirta, T. (1994). Specification, Estimation, and Evaluation of Smooth Transition Autoregressive Models. *Journal of the American Statistical Association 89*(425), 208–218.

Teräsvirta, T. and H. Anderson (1992). Characterizing Nonlinearities in Business Cycles using Smooth Transition Autoregressive Models. *Journal of Applied Econometrics 7*(S1), S119–S136.

Teräsvirta, T. and Y. Yang (2014a). Linearity and Misspecification Tests for Vector Smooth Transition Regression Models. Research Paper 4, CREATES.

Teräsvirta, T. and Y. Yang (2014b). Specification, Estimation and Evaluation of Vector Smooth Transition Autoregressive Models with Applications. Research Paper 8, CREATES.

Tong, H. and K. S. Lim (1980). Threshold Autoregression, Limit Cycles and Cyclical Data. *Journal of the Royal Statistical Society. Series B (Methodological) 42*(3), 245–292.

Tsay, R. (1989). Testing and Modeling Threshold Autoregressive Processes. *Journal of the American Statistical Association 84*(405), 231–240.

Tyssedal, J. and D. Tjøstheim (1988). An Autoregressive Model with Suddenly Changing Parameters and an Application to Stock Market Prices. *Applied Statistics 37*(3), 353–369.

Ubilava, D. (2012). El Niño, La Niña, and World Coffee Price Dynamics. *Agricultural Economics 43*(1), 17–26.

Ubilava, D. (2014). El Niño Southern Oscillation and the Fishmeal–Soya Bean Meal Price Ratio: Regime-Dependent Dynamics Revisited. *European Review of Agricultural Economics 41*(4), 583–604.

Ubilava, D. and C. Helmers (2013). Forecasting ENSO with a Smooth Transition Autoregressive Model. *Environmental Modelling & Software 40*(1), 181–190.

Ubilava, D. and M. Holt (2013). El Niño Southern Oscillation and its Effects on World Vegetable Oil Prices: Assessing Asymmetries using Smooth Transition Models. *Australian Journal of Agricultural and Resource Economics 57*(2), 273–297.

van Dijk, D. and P. Franses (1999). Modeling Multiple Regimes in the Business Cycle. *Macroeconomic Dynamics 3*(3), 311–340.

van Dijk, D., T. Teräsvirta, and P. Franses (2002). Smooth Transition Autoregressive Models – A Survey of Recent Developments. *Econometric Reviews 21*(1), 1–47.

Weise, C. (1999). The Asymmetric Effects of Monetary Policy: A Nonlinear Vector Autoregression Approach. *Journal of Money Credit and Banking 31*(1), 85–108.

Wright, B. D. (2011). The Economics of Grain Price Volatility. *Applied Economic Perspectives and Policy 33*(1), 32–58.

Wright, B. D. (2012). International Grain Reserves and Other Instruments to Address Volatility in Grain Markets. *The World Bank Research Observer 27*(2), 222–260.

Tables

Table 1: Contemporaneous Correlation Between Wheat Prices and the ENSO

	p^{USA}	p^{EUR}	p^{AUS}	p^{CAN}	p^{ARG}
p^{EUR}	0.90^{***}				
p^{AUS}	0.86^{***}	0.82^{***}			
p^{CAN}	0.89^{***}	0.79^{***}	0.73^{***}		
p^{ARG}	0.87^{***}	0.88^{***}	0.76^{***}	0.76^{***}	
ENSO	-0.13^{***}	-0.22^{***}	-0.12^{**}	-0.24^{***}	-0.17^{***}

Note: Table entries are Pearson's correlation coefficients, based on sample size: $T = 396$. Superscripts: *** and ** denote statistical significance at 1% and 5% levels, respectively.

Table 2: Unit Root Test Results

variable	ADF_L	ADF_Δ	ZA_L	ZA_Δ
ENSO	-5.98^{***}	-8.12^{***}	-6.38^{***}	-8.30^{***}
p^{USA}	-3.36^{**}	-9.63^{***}	-4.75^{*}	-9.84^{***}
p^{EUR}	-3.85^{***}	-8.87^{***}	-4.99^{**}	-9.01^{***}
p^{AUS}	-4.76^{***}	-8.80^{***}	-5.26^{**}	-8.93^{***}
p^{CAN}	-3.46^{***}	-9.66^{***}	-5.19^{**}	-10.01^{***}
p^{ARG}	-3.62^{***}	-9.36^{***}	-4.90^{**}	-9.56^{***}

Note: Table entries are the statistics associated with the augmented Dickey–Fuller (ADF) and the Zivot–Andrews (ZA) unit root tests. The sample size is $T = 384$. Subscripts L and Δ identify whether the time series being tested are in levels or in first-differences. Critical values for $\alpha = 0.01$, $\alpha = 0.05$, and $\alpha = 0.10$ significance levels are -3.44, -2.87, and -2.57 in the case of the ADF test statistics, and -5.34, -4.80, and -4.58 in the case of the ZA test statistics. As per convention, superscripts ***, **, and * denote statistical significance at 1%, 5% and 10% levels.

Table 3: Linearity, Parameter Constancy, and Residual Diagnostics

Statistic	ENSO	USA	EUR	AUS	CAN	ARG
H_0 : *Linearity*						
z_{t-1}	<0.001	<0.001	0.111	0.074	<0.001	0.333
z_{t-2}	<0.001	0.095	0.444	0.115	<0.001	0.602
z_{t-3}	<0.001	0.427	0.532	0.578	<0.001	0.435
z_{t-4}	<0.001	0.143	0.297	0.708	<0.001	0.090
H_0 : *Parameter Constancy*						
t^*	0.248	0.051	<0.001	0.006	0.028	0.205
H_0 : *No Remaining Nonlinearity*						
z_{t-1}	0.190	0.034	0.270	0.092	0.003	0.326
z_{t-2}	0.290	0.299	0.661	0.283	0.139	0.576
z_{t-3}	0.184	0.209	0.756	0.814	0.153	0.405
z_{t-4}	0.136	0.018	0.543	0.749	0.044	0.096
H_0 : *No Remaining Parameter Nonconstancy*						
t^*	0.062	0.384	0.651	0.195	0.438	0.400
H_0 : *No Serial Correlation*						
ac_{t-1}	0.028	0.119	0.258	0.670	0.133	0.541
ac_{t-4}	0.245	0.235	0.790	0.403	0.371	0.952
H_0 : *No Conditional Heteroskedasticity*						
$arch_{t-1}$	0.114	0.134	0.080	0.444	0.171	<0.001
$arch_{t-4}$	0.436	0.040	0.453	0.085	<0.001	<0.001

Note: Table entries are asymptotic probability values. The sample size is $T = 384$. The values across z_{t-j}, $j = 1, \ldots, 4$, are those of test statistics associated with the null hypotheses of linearity against STAR-type alternatives (top panel); as well as the null hypotheses of no remaining nonlinearity in the estimated nonlinear models (middle panel). The entries across t^* are probability values of tests statistics associated with null hypotheses of parameter constancy in the estimated linear and nonlinear models (top and middle panels, respectively). The entries across ac_{t-k} and $arch_{t-k}$, $k = 1, 4$, are probability values associated with tests for no remaining residual autocorrelation and no autoregressive conditional heteroskedasticity up to and including lags 1 and 4, respectively.

Table 4: Estimated Parameters of the Transition Functions

Mmeasure	ENSO	USA	EUR	AUS	CAN	ARG
T	384	384	384	384	384	384
k	34	59	59	59	59	37
$\bar{R}^2$	0.938	0.956	0.965	0.956	0.976	0.949
$G(s_t;\gamma,c)$	LSTAR	LSTAR	LTVAR	LTVAR	LSTAR	
s_t	ENSO_{t-3}	ENSO_{t-1}	t/T	t/T	ENSO_{t-1}	
$\hat{\gamma}$	2.21 (0.82)	100 (—)	100 (—)	16.97 (22.58)	4.27 (1.36)	
$\hat{c}$	−0.22 (0.20)	−0.27 (—)	0.60 (—)	0.68 (0.02)	−0.98 (—)	

Note: T denotes sample size; k denotes number of parameters; $\bar{R}^2$ denotes adjusted R-squared. $G(s_t;\gamma,c)$ denotes the type of the estimated transition function, which takes on either the logistic smooth transition autoregressive (LSTAR) or the logistic time-varying autoregressive (LTVAR) form. s_t denotes transition variable, and $\hat{\gamma}$ and $\hat{c}$ denote estimated smoothness and location parameters; the values in the parentheses, underneath the parameter estimates, are asymptotic standard errors. Where the parameters are set, rather than estimated, the standard errors are absent, which is denoted by a dash.

Figures

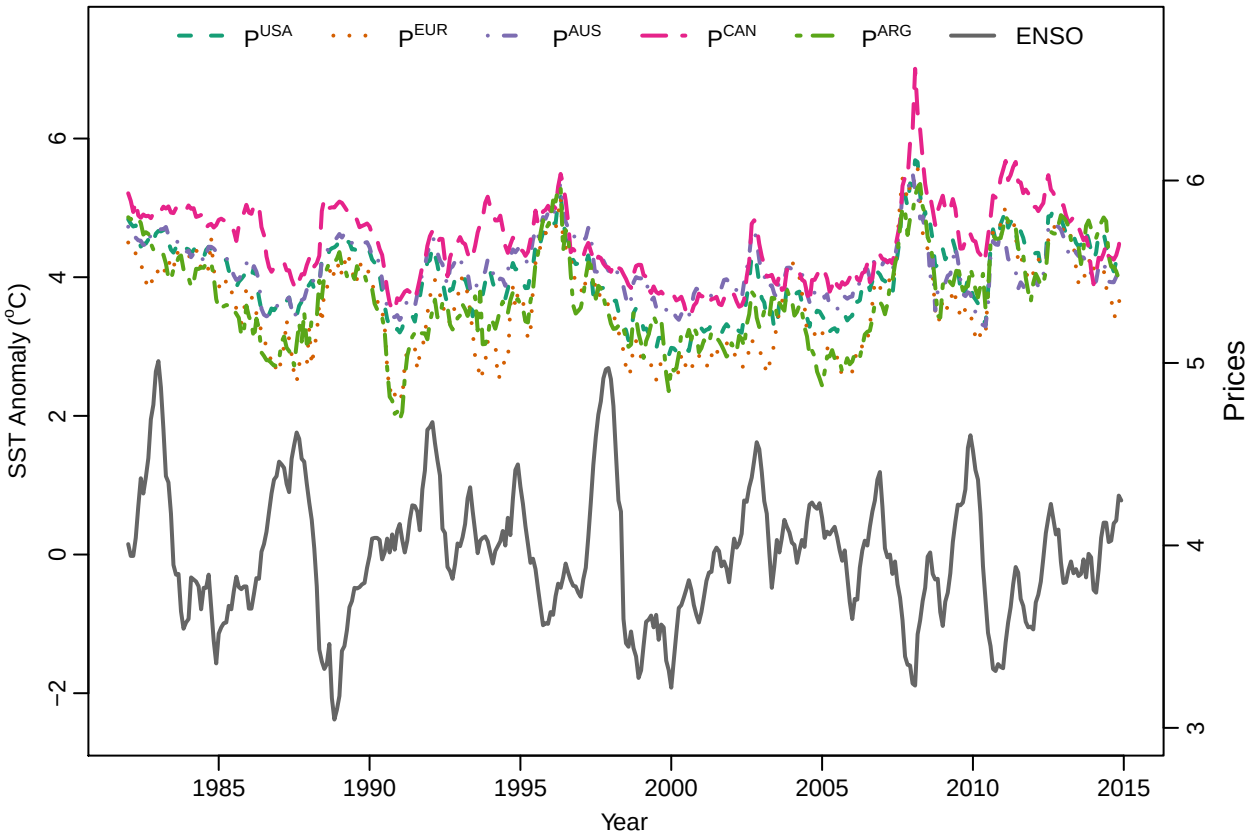

Note: The prices are natural logarithms of real wheat prices.

Figure 1: ENSO and Wheat Prices

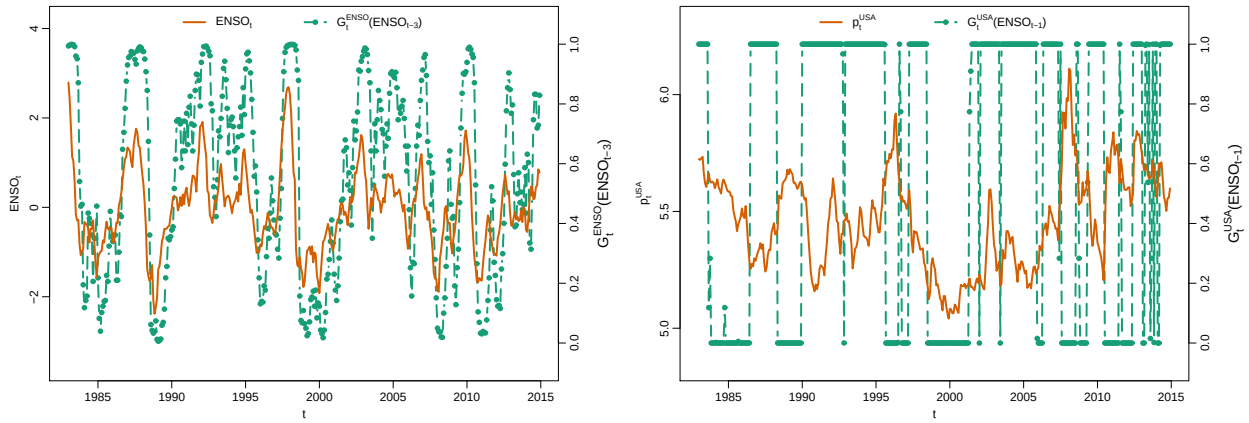

(a) ENSO

(b) USA

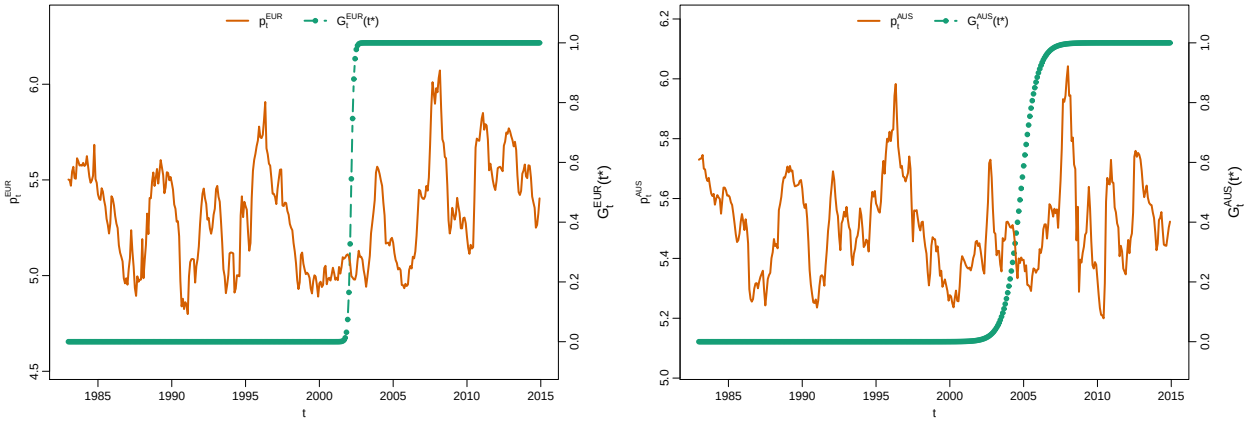

(c) EUR

(d) AUS

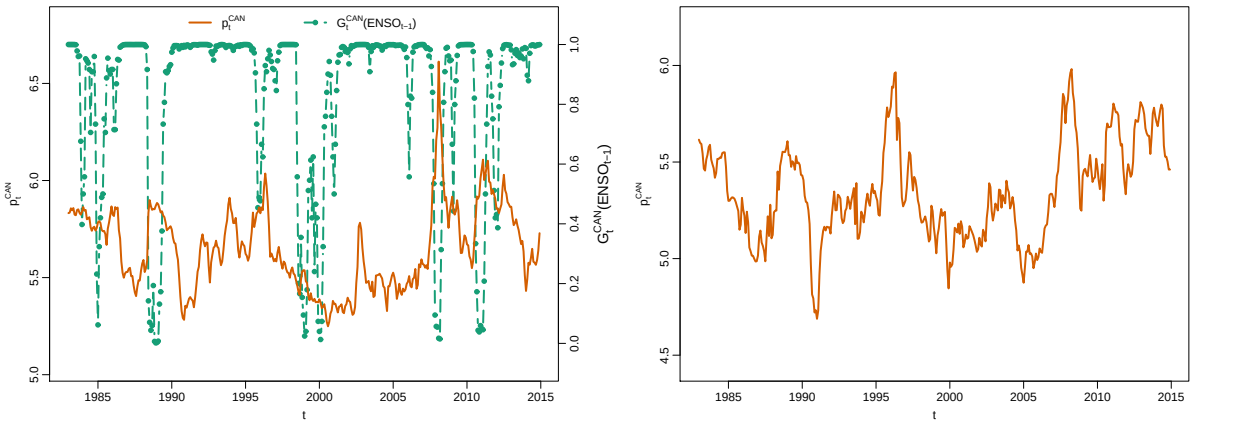

(e) CAN

(f) ARG

Note: The solid orange-red lines are the dependent variables; dashed blue-green lines with dots are the estimated transition functions, $G(s_t)$, where s_t takes on the lagged ENSO variable (panels a, b and e) or the function of time trend, $t^* = t/T$ (panels c and d).

Figure 2: Estimated Transition Functions

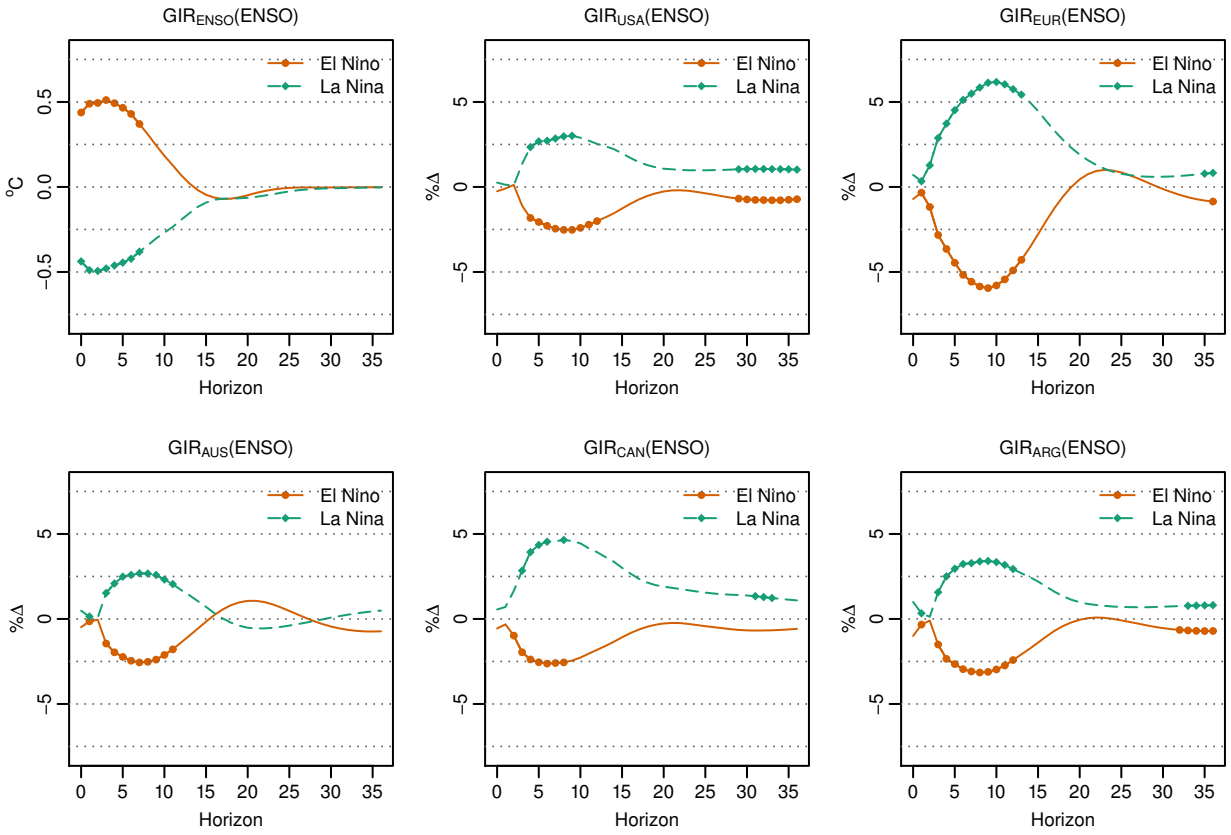

Note: These GIRs are associated with positive (i.e., El Niño-like) and negative (i.e., La Niña-like) shocks, obtained from a randomly sampled history unconditional on past ENSO realizations. $\text{GIR}_{\text{R}}(\text{I})$ denotes the dynamic response of the variable R after a shock to the variable I. In all instances, the effect of (positive and negative) ENSO shocks are considered. GIRs in orange-red (solid lines) are associated with the El Niño shocks, and GIRs in blue-green (dashed line) are associated with the La Niña shocks. Filled circles and diamonds illustrate the statistical significance of GIRs (i.e., when zeros do not fall within the 5th and 95th percentiles of the empirical distribution of GIRs) at a given horizon.

Figure 3: Generalized Impulse–Responses: Overall

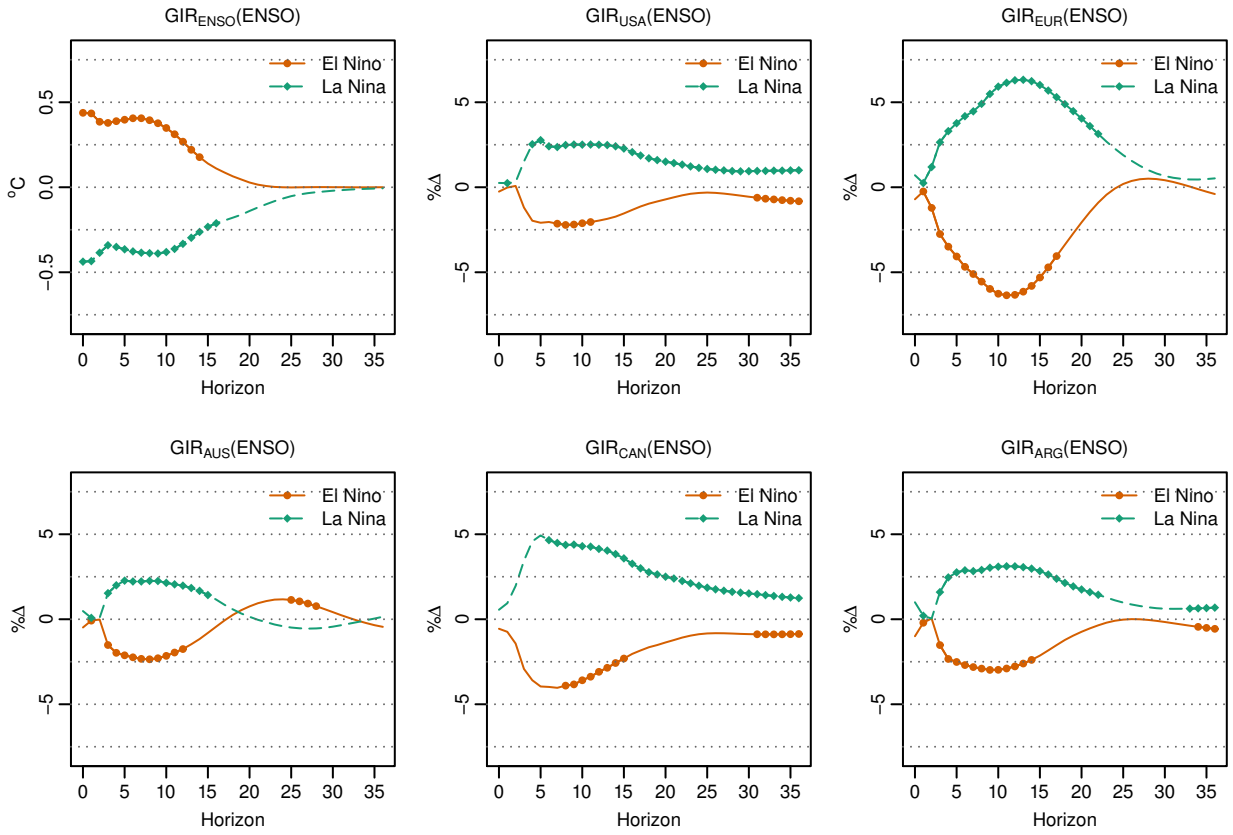

Note: These GIRs are associated with positive (i.e., El Niño-like) and negative (i.e., La Niña-like) shocks, obtained from a randomly sampled subset of histories defined as La Niña conditions. $\text{GIR}_{\text{R}}(\text{I})$ denotes the dynamic response of the variable R after a shock to the variable I. In all instances, the effect of (positive and negative) ENSO shocks are considered. GIRs in orange-red (solid lines) are associated with the El Niño shocks, and GIRs in blue-green (dashed line) are associated with the La Niña shocks. Filled circles and diamonds illustrate the statistical significance of GIRs (i.e., when zeros do not fall within the 5th and 95th percentiles of the empirical distribution of GIRs) at a given horizon.

Figure 4: Generalized Impulse–Responses: La Niña Regime

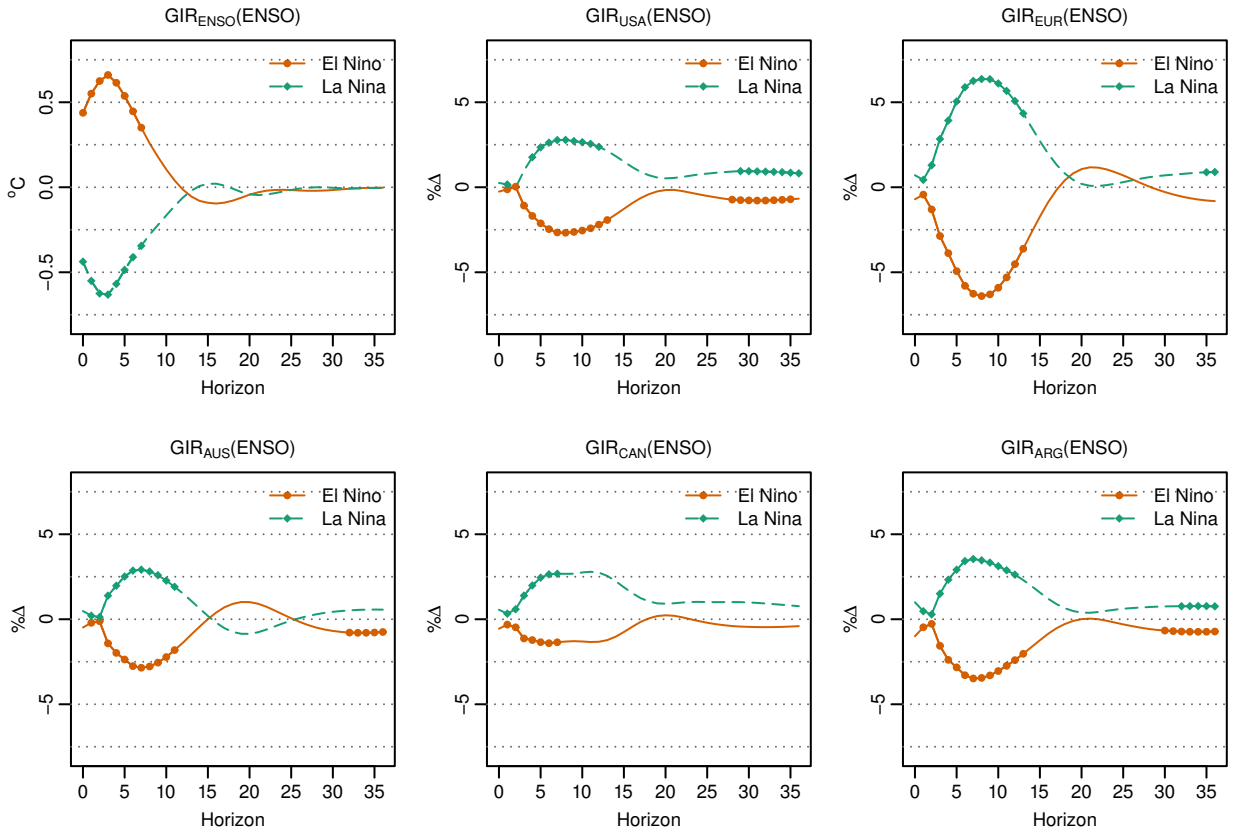

Note: These GIRs are associated with positive (i.e., El Niño-like) and negative (i.e., La Niña-like) shocks, obtained from a randomly sampled subset of histories defined as El Niño conditions. $\text{GIR}_{\text{R}}(\text{I})$ denotes the dynamic response of the variable R after a shock to the variable I. In all instances, the effect of (positive and negative) ENSO shocks are considered. GIRs in orange-red (solid lines) are associated with the El Niño shocks, and GIRs in blue-green (dashed line) are associated with the La Niña shocks. Filled circles and diamonds illustrate the statistical significance of GIRs (i.e., when zeros do not fall within the 5th and 95th percentiles of the empirical distribution of GIRs) at a given horizon.

Figure 5: Generalized Impulse–Responses: El Niño Regime

Appendix

This study applies monthly wheat price series ranging from January of 1982 to December of 2014. The data are collected from the International Grains Council, and are for five major wheat-exporting regions: United States (HRW – Gulf), Europe (France Standard/Grade 1 – Rouen), Australia (ASW – Eastern States), Canada (CWRS – St Lawrence), and Argentina (Trigo Pan – Upriver). Descriptive statistics of these price series are given in Table A.1:

Table A.1: Descriptive Statistics of the Wheat Prices in the Original Data

	Number of Obs.	Mean	Standard Dev.	Skewness	Kurtosis
P_{USA}	396	184.92	73.34	1.35	3.90
P_{EUR}	377	165.65	75.70	1.32	3.94
P_{AUS}	382	184.71	52.09	1.11	3.74
P_{CAN}	387	218.63	86.59	2.04	8.13
P_{ARG}	380	168.65	75.77	1.24	3.44

Several observations are missing in the data. In time series analysis, dropping them is hardly an option. Instead, these missing observations are recovered, in the present case, by taking a simple average of the predicted values obtained using: (i) the cubic spline interpolation method, and (ii) the linear regression of spot prices on the nearby futures prices of the soft red winter wheat as quoted on the Chicago Board of Trade. That is, for a market j in period t for which the spot price, $P_{j,t}$, is unavailable, the reconstructed spot price, $P^r_{j,t}$, is obtained as follows:

$$P^r_{j,t} = 0.5\hat{P}^0_{j,t} + 0.5\hat{P}^*_{j,t} \tag{A.1}$$

where $\hat{P}^0_{j,t}$ is the predicted value from cubic spline interpolation using all available data for the considered price series; and $\hat{P}^*_{j,t} = \exp\left(\hat{p}_{j,t} + \zeta^*_{j,t}\right)$, where $\hat{p}_{j,t}$ is the predicted value obtained from the following static model:

$$p_{j,t} = \mu + \phi p_{f,t} + \boldsymbol{\pi}'\boldsymbol{d}_t + \zeta_{j,t} \tag{A.2}$$

where $p_{j,t} = \ln(P_{j,t})$, and in turn $p_{f,t}$ is the natural logarithm of the wheat futures price in period t; $\boldsymbol{d}_t$ is a vector of seasonal binary variables; and the rest are parameter estimates. Finally, a stochastic component is added to the predicted prices by randomly sampling an idiosyncratic shock, $\zeta^*_{j,t}$, from the pool of the model residuals, $\zeta_{j,t}$, $t = 1, \ldots, T$. Descriptive statistics of the reconstructed price series are given in Table A.2.

Table A.2: Descriptive Statistics of the Wheat Prices in the Reconstructed Data

	Number of Obs.	Mean	Standard Dev.	Skewness	Kurtosis
P_{USA}	396	184.92	73.34	1.35	3.90
P_{EUR}	396	163.33	74.76	1.37	4.13
P_{AUS}	396	189.77	58.84	1.26	4.25
P_{CAN}	396	222.90	90.14	1.84	6.87
P_{ARG}	396	168.90	76.41	1.27	3.56